Hindawi
Journal of Applied Mathematics
Volume 2021, Article ID 7567981, 14 pages
https://doi.org/10.1155/2021/7567981

Research Article

Viscous Dissipation Effect in the Free Convection of Non-Newtonian Fluid with Heat Generation or Absorption Effect on the Vertical Wavy Surface

Mehdi Moslemi[1] **and Kourosh Javaherdeh**[2]

[1]*Department of Mechanical Engineering, Ayandegan Institute of Higher Education, Tonekabon, Iran*
[2]*Faculty of Mechanical Engineering, University of Guilan, Rasht, Iran*

Correspondence should be addressed to Mehdi Moslemi; mehdimoslemi1982@gmail.com

Received 30 April 2021; Revised 7 August 2021; Accepted 18 August 2021; Published 11 October 2021

Academic Editor: Oluwole D. Makinde

The present article analyzes the effect of viscous dissipations on natural convection heat transfer. The power law model for non-Newtonian fluid with heat generation or absorption effect along a sinusoidal wavy surface with isothermal boundary condition is investigated. A simple coordinate transform is employed to map the wavy surface into a flat surface, and also, the fully implicit finite difference method is incorporated for the numerical solution. The findings of this study can help better understand the effect of parameters such as the Brinkman number, heat generation/absorption, wave amplitude magnitude, and generalized Prandtl number on convective heat transfer in dilatant and pseudoplastic non-Newtonian. Results show that as the Brinkman number increases, the amount of heat transfer decreases. This is physically justifiable considering that the fluid becomes warmer due to the viscous dissipation, decreasing its temperature difference with the constant temperature surface. Also, the effect of the power law viscosity index is surveyed. It is demonstrated that the magnitude of the local Nusselt number in the plane leading edge has the smallest quantity for pseudoplastic fluids compared to dilatant Newtonian fluids. Additionally, as the distance from the plane leading edge increases, the heat transfer declines.

1. Introduction

Because of its wide practical application in different contexts, free convection heat transfer of non-Newtonian fluids on the wavy vertical surface has received great attention. However, most previous studies carried out on non-Newtonian fluids have utilized flat surfaces [1, 2]. Since the study of heat transfer from wavy surfaces is more practically widespread and a wavy surface interferes with the development of a boundary layer, thus enhancing the heat transfer in the applications such as solar collectors and condensers, this article is aimed at further understanding their heat transfer characteristics.

One of the early researches on the free convection heat transfer of non-Newtonian fluids on wavy surfaces accompanied by the magnetic effect is accomplished by Yang et al. [3]. They solved a converted set of equations by the cubic spline method and showed that the temperature gradient for dilatant fluids is more than that for pseudoplastic fluids. Kim [4] numerically investigated the natural convection along a vertical wavy plate for non-Newtonian fluids. He analyzed the effect of parameters like flow index, Prandtl number, and surface amplitude on the velocity and thermal boundary layer. His results show that the effect of wavy geometry is large in the starting edge of the surface and it gradually decreases. Also, when the natural convection boundary layer grows thick, the local Nusselt number decreases. Chen and Wang [5] studied the transient laminar-forced convection heat transfer of micropolar fluids on wavy surfaces. Applying mapping of the wavy surface onto the flat surface, they proceeded with solving boundary layer equations by a spline alternating-direction implicit method. They showed that with the increase in surface wave length and amplitude, the local Nusselt number and skin

friction tend to increase. Their findings showed that the thickness of temperature and velocity boundary layer increase with time. The mixed convection heat transfer of non-Newtonian fluid along wavy surfaces was studied by Wang and Chen [6]. Using the cubic spline collocation numerical method, they found out that the heat flux for wavy surfaces is more than that of the flat plate; also, for a given Richardson number, higher wavy amplitude wavelength ratio and Prandtl number correspond to higher heat transfer. Jang and Yan [7] solved for coupled heat and mass transfer for mixed convection on a vertical wavy plate. They incorporated a marching finite difference method and demonstrated that by increasing the Richardson number, the effect of buoyancy on heat and mass transfer increases which means that natural convection is dominated in the studied mixed convection flow.

The effect of internal heat generation/absorption in the natural convection heat transfer on wavy surfaces was investigated by Molla et al. [8]. The Nusselt number decreases in the downstream for both heat generation and absorption as their results show. Wang and Chen [9] investigated the mixed convection heat transfer accompanied by magnetohydrodynamic effect for different angles of wavy surfaces. They found that the increase in inclined angle, amplitude-wavelength ratio, and Richardson number tends to increase the buoyancy effect, thus enhancing the heat transfer while increasing the skin friction. Moreover, the magnetic field accelerates the flow in the leading edge and decelerates it downstream. MHD effect and natural convection with heat generation or absorption along a vertical wavy surface have been studied by Hady et al. [10]. They utilized the Runge-Kutta integration scheme for solving the nonlinear boundary layer equations.

The study of heat generation or absorption in non-Newtonian fluids is important in problems dealing with chemical reactions and those concerned with dissociating fluids. Vajravelu and Hadjinicolaou [11] studied the heat transfer characteristic in the laminar boundary layer of a viscous fluid over a stretching sheet with viscous dissipation or frictional heating and internal heat generation. It is worth mentioning here that in the current study, we have set (according to Hady et al. [10]) the volumetric rate of heat generation, q''' ($\mathrm{W \cdot m^{-3}}$), as follows:

$$q'' = \begin{cases} Q_0(T - T_\infty), & T > T\infty, \\ 0, & T < T\infty, \end{cases} \tag{1}$$

where Q_0 is the heat generation/absorption constant. The above relation is comprehensively explained by Vajravelu and Hadjinicolaou.

Molla and Yao [12] used a modified power law viscosity model to analyze the natural convection of non-Newtonian fluids along a vertical wavy surface. Mirzaei Nejad et al. [13] investigated the effect of a magnetic field on the heat transfer of power law fluids over a vertical wavy plate. They showed that the magnetic field competes against the buoyancy force effects.

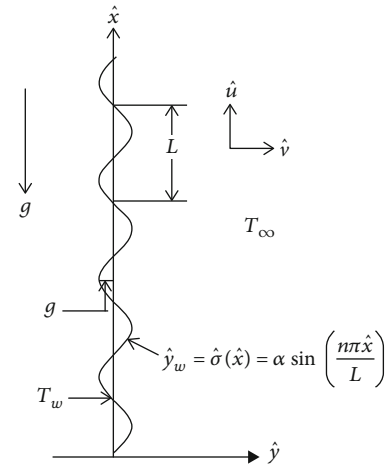

Figure 1: The physical model and the coordinate system of the problem.

Unsteady natural convection heat and mass transfer of non-Newtonian fluids obtained by Mahdy and Ahmed [14]. They found that by increasing the caisson parameter or the buoyancy ratio, the values of the local Nusselt and Sherwood numbers increase.

Rath and Dash [15] carried out the effect of Prandtl number on natural convection from a wavy vertical plate in non-Newtonian power law fluids. They showed that the heat transfer coefficient was directly dependent on both Prandtl and Grashef numbers. Hady et al. [16] presented unsteady natural convection of the non-Newtonian caisson fluid model considering the dusty particles in the boundary layer on a vertical wavy plate. They found that when the fluid-particle interaction parameter enhances, fluid velocity decreases and enhances the velocity and temperature of the particle phase.

Additionally, since non-Newtonian fluids have high viscosity and high Prandtl numbers, the effect of the viscous dissipation would be considerable. Moreover, up to the present time, in the researches performed regarding non-Newtonian fluids, there has been little attention to the effect of the viscous dissipation; thus, the novelity of this article is the investigation of the influence of viscous dissipation in free convection heat transfer of non-Newtonian fluid with heat generation or absorption on a vertical wavy surface, in which the surface temperature is more than the ambient temperature.

In the sections that follows: first, the mathematical formulation is presented; second, a simple coordinate transform is applied to convert the wavy surface to a flat one, and then the transformed boundary layer equations have been solved with the finite difference method.

The influence of parameters such as the Brinkman number, generation or absorption of heat, magnitude of the wave amplitude, and generalized Prandtl number in the form of the local Nusselt number and the profiles of temperature and velocity has been studied.

2. Mathematical Formulation

The boundary layer stream of desired fluid passes on a semi-infinite body having a vertical wavy surface. The vertical

wavy surface is defined as $\sigma(\bar{x}) = \bar{a}\sin(n\pi x/L)$ in which $\bar{a}$ is the wave amplitude and L is the length of a wave. The surface temperature of the wavy body has a constant value of T_w, which is greater than the ambient temperature T_∞. The free surface velocity and the input velocity (the plane leading edge) are equal to zero. Figure 1 shows the physical model and the coordinate system of the problem. In this coordinate system, x is located along the longitudinal wavy planes in the same direction as the fluid stream, while y is perpendicular to the stream.

The fluid stream is laminar, incompressible, steady, and two-dimensional; thus, considering the viscous dissipation and heat generation or absorption effect, the governing equations are as follows:

$$\frac{\partial \bar{u}}{\partial \bar{x}} + \frac{\partial \bar{v}}{\partial \bar{y}} = 0, \tag{2}$$

$$\rho\left(\bar{u}\frac{\partial \bar{u}}{\partial \bar{x}} + \bar{v}\frac{\partial \bar{u}}{\partial \bar{y}}\right) = -\frac{\partial \bar{p}}{\partial \bar{x}} + \left(\frac{\partial \tau_{\bar{x}\bar{x}}}{\partial \bar{x}} + \frac{\partial \tau_{\bar{x}\bar{y}}}{\partial \bar{y}}\right) + \rho g\beta(T - T_\infty), \tag{3}$$

$$\rho\left(\bar{u}\frac{\partial \bar{v}}{\partial \bar{x}} + \bar{v}\frac{\partial \bar{v}}{\partial \bar{y}}\right) = -\frac{\partial \bar{p}}{\partial \bar{y}} + \left(\frac{\partial \tau_{\bar{y}\bar{x}}}{\partial x} + \frac{\partial \tau_{\bar{y}\bar{y}}}{\partial \bar{y}}\right), \tag{4}$$

$$\rho C_p\left(\bar{u}\frac{\partial T}{\partial \bar{x}} + \bar{v}\frac{\partial T}{\partial \bar{y}}\right) = K\left(\frac{\partial^2 T}{\partial \bar{x}^2} + \frac{\partial^2 T}{\partial \bar{y}^2}\right) + Q_0(T - T_\infty) + \Phi, \tag{5}$$

where Φ is a term due to viscous dissipation, and it is equal to

$$\Phi = \mu_{\text{apr}}\left\{2\left(\frac{\partial \bar{u}}{\partial \bar{x}}\right)^2 + 2\left(\frac{\partial \bar{v}}{\partial \bar{y}}\right)^2 + \left(\frac{\partial \bar{u}}{\partial \bar{y}} + \frac{\partial \bar{v}}{\partial \bar{x}}\right)^2\right\}^2. \tag{6}$$

μ_{apr} is the apparent viscosity of the non-Newtonian fluid which is equal to

$$\mu_{\text{apr}} = m\left\{2\left(\frac{\partial \bar{u}}{\partial \bar{x}}\right)^2 + 2\left(\frac{\partial \bar{v}}{\partial \bar{y}}\right)^2 + \left(\frac{\partial \bar{u}}{\partial \bar{y}} + \frac{\partial \bar{v}}{\partial \bar{x}}\right)^2\right\}^{(n-1)/2}. \tag{7}$$

The boundary conditions existing in the problem are as follows:

(1) On the wavy surface: $T = T_w \quad \bar{u} = \bar{v} = 0$

(2) On the free surface: $\bar{y} \longrightarrow \infty$, $T \longrightarrow T_\infty$, $\bar{u} = 0$

In the above equations, $\bar{u}$ and $\bar{v}$ are the fluid velocity vectors in the $\bar{x}$ and $\bar{y}$ directions, ρ is the density, $\bar{p}$ is the pressure, C_p is the specific heat capacity at the constant pressure, and T and β are the fluid temperature and the coefficient of thermal diffusion, respectively. The amount of heat generated or absorbed per unit volume is $Q_0(T - T_\infty)$, with Q_0 being a constant, which may take either positive or negative values. The source term represents the heat generation when $Q_0 > 0$ and the heat absorption when $Q_0 < 0$.

Using the Prandtl transform to convert the wavy surface to a flat one, the dimensionless variables for making the equations dimensionless are as follows [4, 6]:

$$x^* = \frac{x}{L}, y^* = \frac{y - \bar{\sigma}}{L}\text{Gr}_g^{1/(2(n+1))}, u^* = \frac{\bar{u}}{\sqrt{Lg\beta\Delta T}}, \sigma = \frac{\bar{\sigma}}{L},$$

$$v^* = \frac{\left(\bar{v} - \sigma'\bar{u}\right)}{\sqrt{Lg\beta\Delta T}}\text{Gr}_g^{1/(2(n+1))}, \theta = \frac{T - T_\infty}{T_w - T_\infty}, p^* = \frac{\bar{p}}{\rho Lg\beta\Delta T},$$

$$\text{Pr}_g = \frac{\rho C_p}{K_f}\left(\frac{m}{\rho}\right)^{2/(1+n)}, \text{Gr}_g = \frac{\rho^2 L^{n+2}[\beta g\Delta T]^{2-n}}{m^2}, Q = \frac{Q_0 L}{\rho C_p\sqrt{Lg\beta\Delta T}}. \tag{8}$$

Using the boundary layer approximation and introducing dimensionless variables in equations (2)–(5), we will have what follows [6]:

$$\frac{\partial u^*}{\partial x^*} + \frac{\partial v^*}{\partial y^*} = 0, \tag{9}$$

$$u^*\frac{\partial u^*}{\partial x^*} + v^*\frac{\partial u^*}{\partial y^*} = -\frac{\partial p^*}{\partial x^*} + \sigma'\frac{\partial p^*}{\partial y^*}\text{Gr}_g^{1/(2(n+1))} + \left(1 + \sigma'^2\right)^n\frac{\partial}{\partial y^*} \cdot \left(\frac{\partial u^*}{\partial y^*}\left|\frac{\partial u^*}{\partial y^*}\right|^{(n-1)}\right) + \theta, \tag{10}$$

$$u^{*2}\sigma'' + \sigma'\theta = \sigma'\frac{\partial p^*}{\partial x^*} - \left(1 + \sigma'^2\right)\frac{\partial p^*}{\partial y^*}\text{Gr}_g^{1/(2(n+1))}, \tag{11}$$

$$u^*\frac{\partial \theta}{\partial x^*} + v^*\frac{\partial \theta}{\partial y^*} = \frac{1}{\text{Pr}_g}\left(1 + \sigma'^2\right)\frac{\partial^2\theta}{\partial y^{*2}} + \frac{\text{Br}}{\text{Pr}_g} \cdot \left(1 + \sigma'^2\right)^{n+1}\left|\frac{\partial u^*}{\partial y^*}\right|^{(n+1)} + Q\theta. \tag{12}$$

As it is shown, the pressure gradient in the y direction has order $O(\text{Gr}_g^{-1/(2(n+1))})$ and the pressure gradient in the x direction are obtained by solving the inviscid flow. By neglecting the pressure gradient in the x direction and eliminating $\partial p^*/\partial y^*$ using equations (10) and (11) in the present problem, the momentum equation could be written as one equation; thus [6],

$$u^*\frac{\partial u^*}{\partial x^*} + v^*\frac{\partial u^*}{\partial y^*} = \frac{1}{\left(1 + \sigma'^2\right)}\left(\theta - u^{*2}\sigma'\sigma''\right) + \left(1 + \sigma'^2\right)^n\frac{\partial}{\partial y^*} \cdot \left(\frac{\partial u^*}{\partial y^*}\left|\frac{\partial u^*}{\partial y^*}\right|^{(n-1)}\right). \tag{13}$$

Since the point $x^* = 0$ is a singular point, to remove it, we use the following transforms:

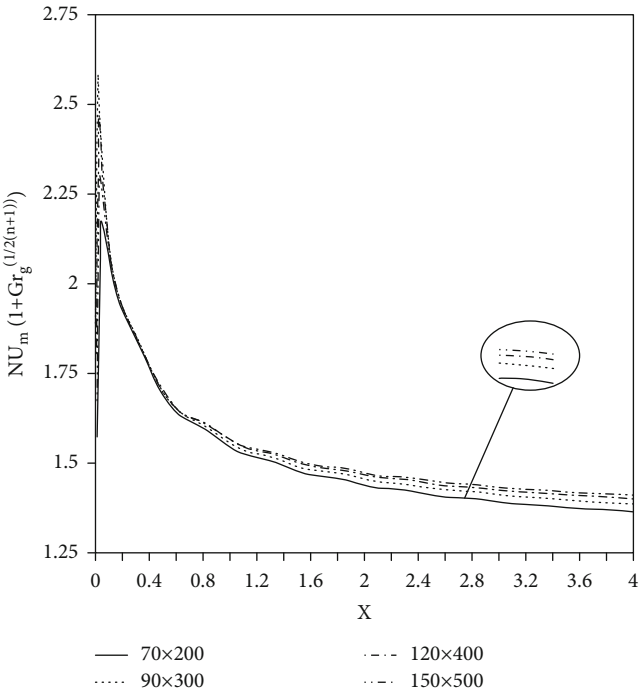

Figure 2: Mean Nusselt number for the grid independence test.

$$X = x^*\,;\, Y = \frac{y^*}{\left[2(n+1)x^*\right]^{1/(2(n+1))}}, \tag{14}$$

$U = u^*/\left[2(n+1)x^*\right]^{1/2n}\,;\, V = \left[2(n+1)x^*\right]^{1/(2(n+1))}v^*.$

By placing equation (14) into equations (9), (12), and (13), the final equations will be as follows:

$$\frac{n+1}{n}U + [2(n+1)X]\frac{\partial U}{\partial X} - Y\frac{\partial U}{\partial Y} + [2(n+1)X]^{((n-1)(2n+1))/(2n(n+1))}\frac{\partial V}{\partial Y} = 0, \tag{15}$$

$$[2(n+1)X]^{1/n}U\frac{\partial U}{\partial X} + \left\{[2(n+1)X]^{(1-n)/(2n(n+1))}V - [2(n+1)X]^{(1-n)/n}UY\right\}\frac{\partial U}{\partial Y} = -\left(\frac{n+1}{n}[2(n+1)X]^{(1-n)/n} + \frac{\sigma'\sigma''[2(n+1)X]^{1/n}}{1+\sigma'^2}\right)U^2 + \frac{1}{1+\sigma'^2}\theta + \left(1+\sigma'^2\right)^n\frac{\partial}{\partial Y}\left(\frac{\partial U}{\partial Y}\left|\frac{\partial U}{\partial Y}\right|^{(n-1)}\right), \tag{16}$$

$$[2(n+1)X]^{(3n+1)/[2n(n+1)]}U\frac{\partial\theta}{\partial X} + \left(V - [2(n+1)X]^{((1-n)(1+2n))/(2n(1+n))}UY\right)\times\frac{\partial\theta}{\partial Y} = \frac{1}{\mathrm{Pr}_g}\left(1+\sigma'^2\right)\frac{\partial^2\theta}{\partial Y^2} + \frac{Br}{\mathrm{Pr}_g}\left(1+\sigma'^2\right)^{(n+1)}\cdot[2(n+1)X]^{3n/(2n(n+1))}\left|\frac{\partial U}{\partial Y}\right|^{(n+1)} + [2(n+1)X]^{1/(n+1)}, \tag{17}$$

where the boundary conditions are as follows:

(1) In $y = 0\,\theta = 1, u = v = 0$

Table 1: Comparison of the Nusselt number as $\mathrm{Nu}_x[2n+1X\mathrm{Gr}_g]$ $1/2(n+1)$ with other results for $\alpha = 0.10$, $\mathrm{Pr}_g = 1.0$, and $n = 1$.

Present	Kumari et al. [17]	Chiu and Chou [18]	X
0.533551	0.53634	0.535919	1.5
0.535451	0.54810	0.562036	1.75
0.533588	0.53709	0.534797	2.0
0.544652	0.54732	0.562414	2.25
0.533216	0.53762	0.533628	2.5

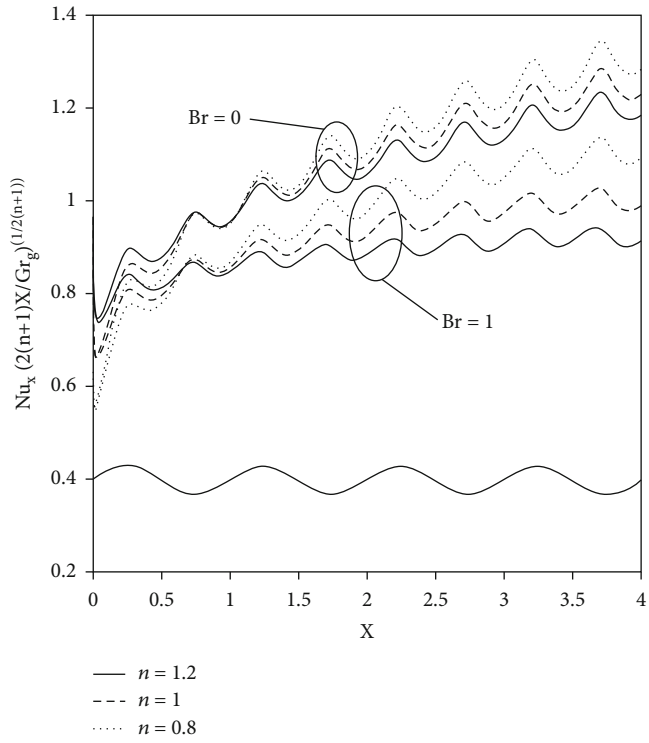

Figure 3: The axial distribution of the local Nusselt number for $\mathrm{Pr}_g = 2$, $\alpha = 0.2$, Br = 0 − 1, n = 1.2-1.0-0.8, and $Q = -0.2$.

(2) In $y \longrightarrow \infty\,\theta \longrightarrow 0, u \longrightarrow 0$

Using Newton's cooling law and the necessary transforms, one can determine the following terms for the local Nusselt number and the mean Nusselt number:

$$\mathrm{Nu}_{\bar{x}} = -\left[\mathrm{Gr}_g/2(n+1)X\right]^{1/2(n+1)}\left(1+S'^2\right)^{1/2}\left.\frac{\partial\theta}{\partial Y}\right|_{Y=0}. \tag{18}$$

Also, the mean Nusselt number can be obtained from the following formulation:

$$\mathrm{Nu}_m = -\frac{1}{S}\int_0^x\left[\frac{\mathrm{Gr}_g}{2(n+1)X}\right]^{1/2(n+1)}\left(1+S'^2\right)\left.\frac{\partial\theta}{\partial Y}\right|_{Y=0}dX, \tag{19}$$

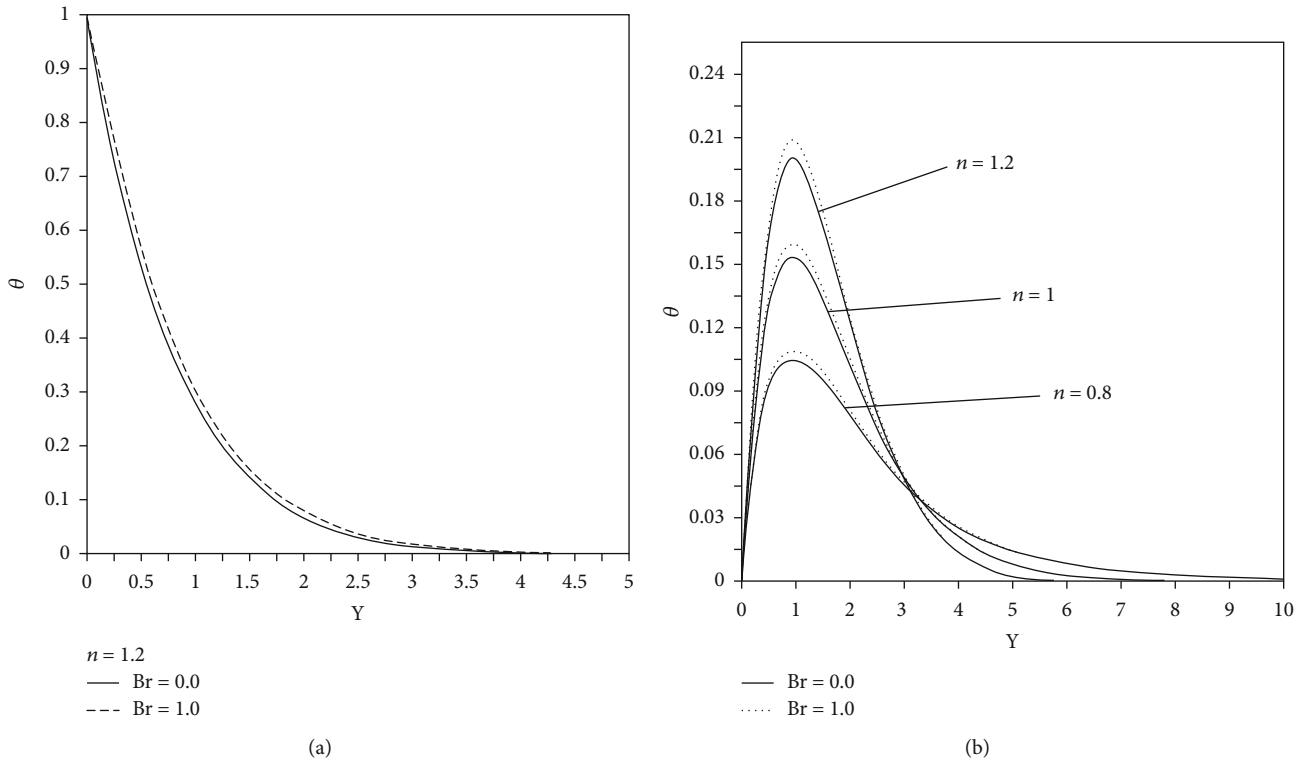

FIGURE 4: (a) Thermal profile and (b) velocity profile for $\mathrm{Pr_g} = 2.0$, $\alpha = 0.2$, $Br = 0 - 1$, and $Q = -0.2$ in $x = 3.75$.

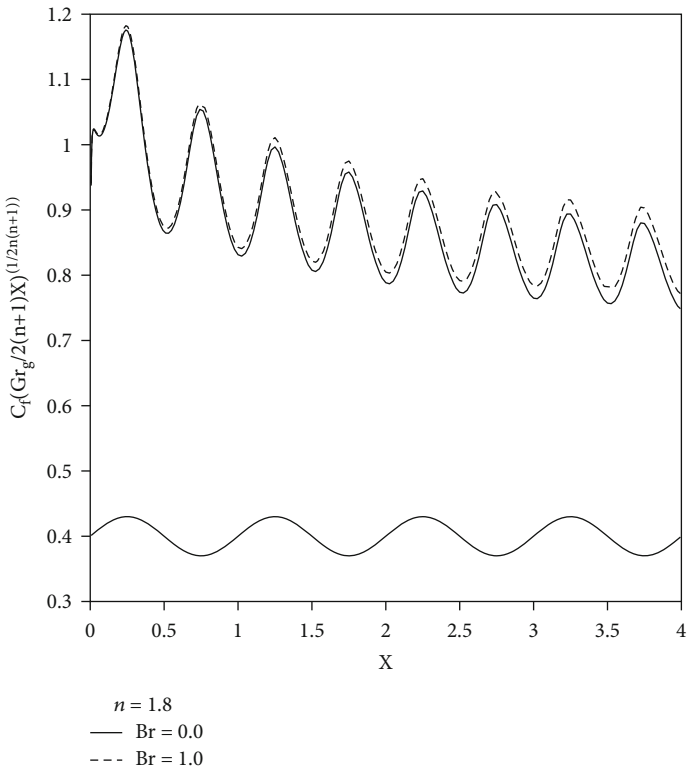

FIGURE 5: The axial distribution of the skin friction coefficient for $\mathrm{Pr_g} = 2$, $\alpha = 0.2$, Br = 0-1, $n = 0.8$, and $Q = -0.2$.

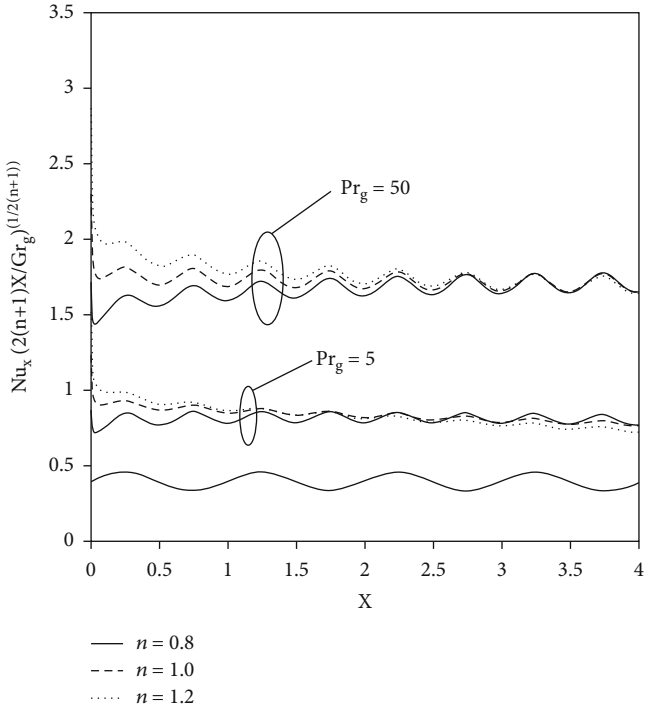

Figure 6: The axial distribution of the local Nusselt number for $P = 5\text{-}50$, $\alpha = 0.1$, Br = 0.5, and $n = 1.2\text{-}1.0\text{-}0.8$.

where.

$$S = \int_0^x \left(1 + S'^2\right)^{1/2} dx. \tag{20}$$

The friction factor is defined as follows:

$$C_f = \frac{2\tau_w}{\rho \tilde{U}^2}, \tag{21}$$

where.

$$\tilde{U} = Lg\beta\Delta T, \tag{22}$$

where $\tilde{U}$ is the characteristic of velocity. Therefore, the dimensionless equation of the friction factor is

$$C_f = 2[2(n+1)X]^{1/2n(n+1)} \left(\frac{1}{\mathrm{Gr_g}}\right)^{1/2(n+1)} \left(1 + S'^2\right)^n \left(\frac{\partial u}{\partial y}\right)^n \Bigg|_{y=0}. \tag{23}$$

3. Numerical Solution Method

The viscous fluid flow has a larger velocity gradient near the wavy wall in the y direction and also near the leading edge in the x direction. Thus, we used the following transforms{Lin, 2009 #11} in order to achieve a nonuniform grid with smaller spacing of mesh points near the fluid-solid boundary in the y direction and near the leading edge in the x direction.

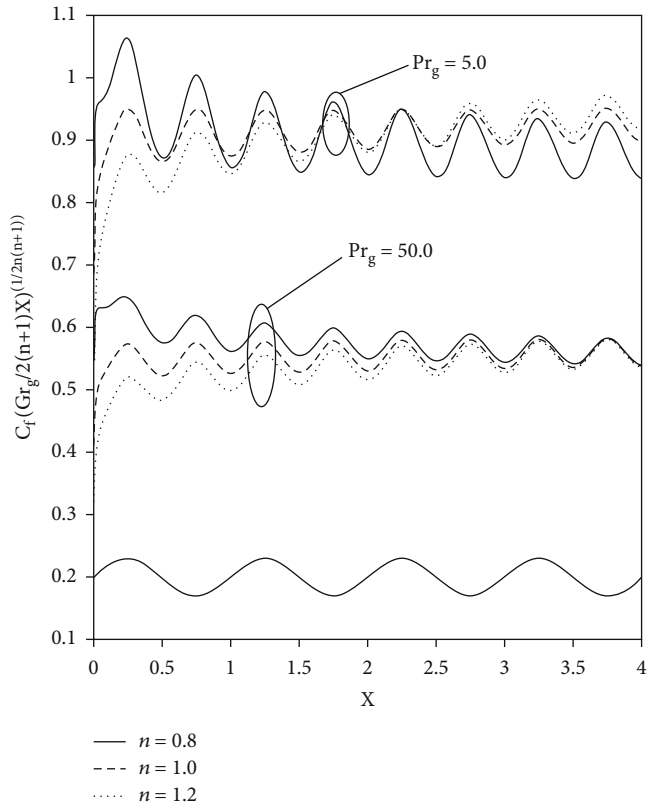

Figure 7: The axial distribution of the skin friction coefficient for $P = 5\text{-}50$, $\alpha = 0.1$, Br = 0.5, $Q = 0$, and $n = 1.2\text{-}1.0\text{-}0.8$.

$$Y = H\frac{(\beta+1)-(\beta-1)\left\{[(\beta+1)/(\beta-1)]^{1-\eta}\right\}}{[(\beta+1)/(\beta-1)]^{1-\eta}+1}, \tag{24}$$

$$X = L\frac{\left(\beta'+1\right)-\left(\beta'-1\right)\left\{\left[\left(\beta'+1\right)/\left(\beta'-1\right)\right]^{1-\xi}\right\}}{\left[\left(\beta'+1\right)/\left(\beta'-1\right)\right]^{1-\zeta}+1}. \tag{25}$$

In this equation, β and β' are the clustering parameters. When their value approaches to 1, more grid points are near the surface and leading edge subsequently.

Substituting equations (24) and (25) into in the dimensionless equations (15)–(17) and using the fully implicit finite difference numerical method, as in the diffusion and transverse heat transfer, we utilized central difference discretization, and in axial heat transfer, the backward difference method using upstream flow has been applied. The governing equations are considered unstable until the flow regime reaches a stable state.

The discretized equations are as follows:

Momentum equation to obtain U:

$$\begin{aligned}
&[2(n+1)X]^{1/n}U_{i,j}^{n}\frac{U_{i,j}^{n+1}-U_{i-1,j}^{n}}{\Delta\xi}\xi_X \\
&+\left\{[2(n+1)X_i]^{(1-n)/(2n(n+1))}V_{i,j}^{n}-[2(n+1)X_i]^{(1-n)/n}U_{i,j}^{n}Y_j\right\} \\
&\times\frac{U_{i,j+1}^{n+1}-U_{i,j-1}^{n+1}}{2\Delta\eta}\eta_Y=\left(\frac{n+1}{n}[2(n+1)X_i]^{(1-n)/n}+\frac{\sigma'\sigma''[2(n+1)X_i]^{1/n}}{1+\sigma'^2}\right)U_{i,j}^{n}U_{i,j}^{n+1} \\
&+\frac{1}{1+\sigma'^2}\theta_{i,j}^{n}+n\left(1+\sigma'^2\right)^{n}\left|\frac{U_{i,j+1}^{n}-U_{i,j-1}^{n}}{\Delta\eta}\eta_Y\right|^{(n-1)} \\
&\times\left[\frac{U_{i,j+1}^{n+1}-2U_{i,j}^{n+1}+U_{i,j-1}^{n+1}}{\Delta\eta^2}\eta_Y{}^2+\frac{U_{i,j+1}^{n+1}-U_{i,j-1}^{n+1}}{2\Delta\eta}\eta_{YY}\right].
\end{aligned} \tag{26}$$

Equation of continuity to obtain V:

$$\begin{aligned}
&\frac{n+1}{n}U_{i,j}^{n}+[2(n+1)X_i]\frac{U_{i,j}^{n+1}-U_{i-1,j}^{n}}{\Delta\xi}\xi_X-Y_j\frac{U_{i,j+1}^{n+1}-U_{i,j-1}^{n+1}}{2\Delta\eta}\eta_Y \\
&\qquad+[2(n+1)X]^{((n-1)(2n+1))/(2n(n+1))}\frac{V_{i,j+1}^{n+1}-V_{i,j}^{n}}{\Delta\eta}\eta_Y=0.
\end{aligned} \tag{27}$$

Energy equation to obtain θ:

$$\begin{aligned}
&[2(n+1)X_i]^{(3n+1)/[2n(n+1)]}U_{i,j}^{n}\frac{\theta_{i,j}^{n+1}-\theta_{i-1,j}^{n}}{\Delta\xi}\xi_X \\
&\quad+\left(V_{i,j}^{n}-[2(n+1)X_i]^{((1-n)(1+2n))/(2n(1+n))}U_{i,j}^{n}Y_j\right)\frac{\theta_{i,j+1}^{n+1}-\theta_{i,j-1}^{n+1}}{2\Delta\eta}\eta_Y \\
&=\frac{1}{\mathrm{Pr}_g}\left(1+\sigma'^2\right)\frac{\theta_{i,j+1}^{n+1}-2\theta_{i,j}^{n+1}+\theta_{i,j-1}^{n+1}}{\Delta\eta^2}\eta_Y{}^2+\frac{\mathrm{Br}}{\mathrm{Pr}_g}\left(1+\sigma'^2\right)^{(n+1)} \\
&\quad\cdot[2(n+1)X_i]^{3n/(2n(n+1))}\left|\frac{U_{i,j+1}^{n}-U_{i,j-1}^{n}}{\Delta\eta}\eta_Y\right|^{(n+1)} \\
&\quad+[2(n+1)X]^{1/(n+1)}Q\theta_{i,j}^{n+1}.
\end{aligned} \tag{28}$$

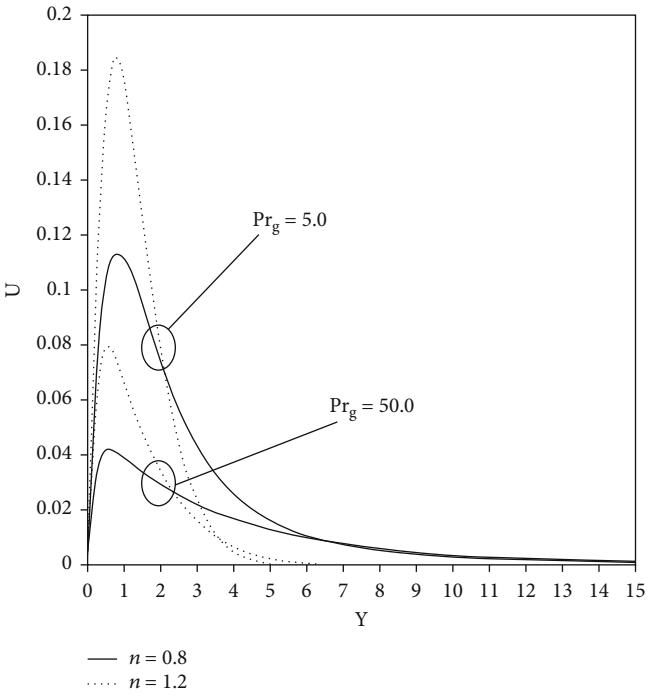

Figure 8: Velocity profile for $\alpha = 0.1$, Br = 0.5, n = 1.2-0.8, and Q = 0.

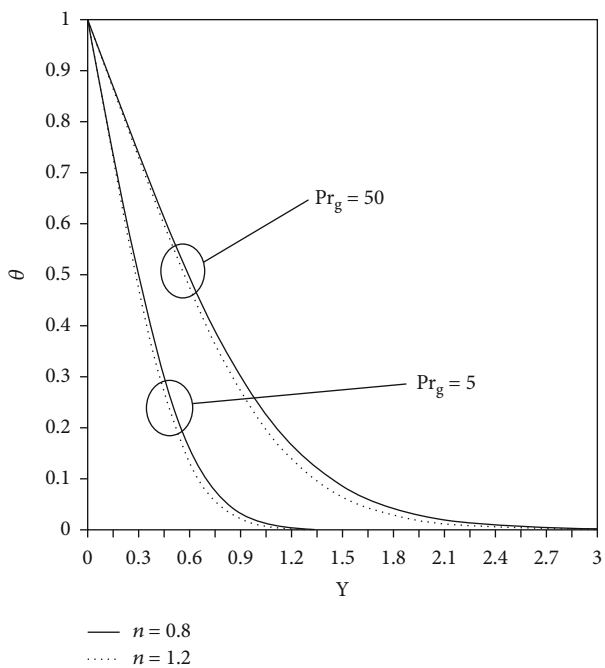

Figure 9: Thermal profile for $\alpha = 0.1$, Br = 0.5, n = 1.2-0.8, and Q = 0.

After separation, the algebraic equations are written as a three-diagonal matrix as follows:

$$A_{i,j}\Omega^{n+1}{}_{i,j-1}+B_{i,j}\Omega^{n+1}{}_{i,j}+C_{i,j}\Omega^{n+1}{}_{i,j+1}=D_{i,j}, \tag{29}$$

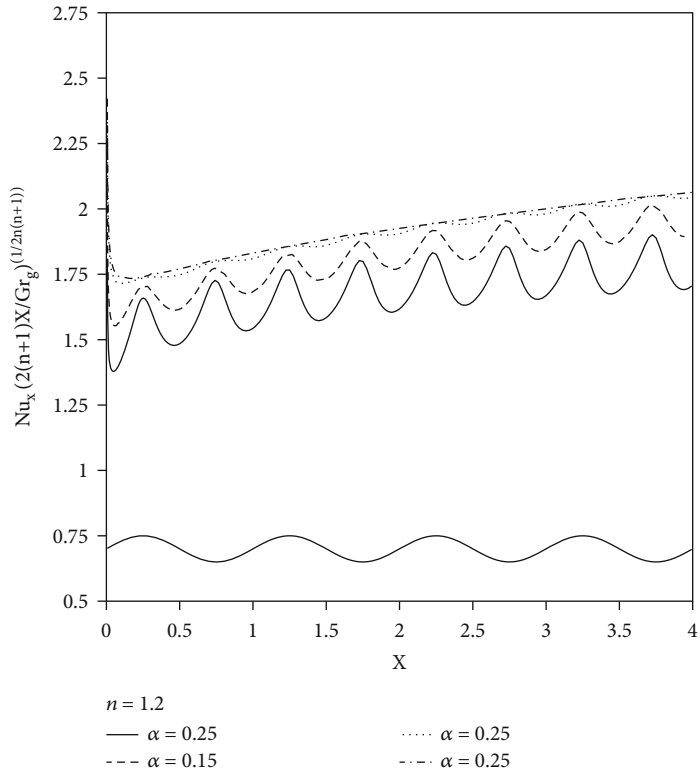

FIGURE 10: The axial distribution of the local Nusselt number for $Pr_g = 20$, Br = 0.7, $n = 1.2$, and $Q = -0.05$.

where U and θ replace Ω. Equation (29) is in the three-diagonal form, which can be easily solved through the Thomas algorithm. The solution of the equations will be continued as much as the convergence limit is obtained. The convergence limit has the following form:

$$\frac{\Omega_{i,j}^{n+1} - \Omega_{i,j}^{n}}{\Omega_{\max}^{n}} < 5 \times 10^{-5}. \quad (30)$$

4. Results and Discussions

In the present problem, considering that the temperature and velocity gradient changes in the vicinity of the wavy plane in the y direction and also in the vicinity of the plane leading edge in the x direction are more than those in other positions, we use a finer mesh for the mentioned areas.

The very important problem in the numerical simulation is to make sure of having sufficient number of mesh points. To achieve proper and sufficient points in practice, the calculations are commenced with a proper mesh, and then, the mesh number of points is gradually increased so that after reaching a proper point number, the influence of the mesh on the results becomes negligible. For the aforesaid problem meshes of 70×200, 90×300, 120×400, and 150×500, dimensions have been analyzed, and the obtained results in Figure 2 show that for the mean Nusselt number, the discrepancy between meshes (120×400 and 150×500) is less than 0.2%.

In Table 1, current results are compared to those obtained by Kumari et al. [17] and Chiu and Chou [12, 18] on Newtonian fluid. Obviously, the obtained results are very similar and compatible with their results.

In Figure 3, the axial distribution of the local Nusselt number for $Pr_g = 2$, $\alpha = 0.2$, $n = 1.2$-1-0.8, $Q = -0.2$, and Br = 0-1 has been shown. It is clear that the increase in the Brinkman number and the effect of viscous dissipations cause the fluid to warm up more and to increase in temperature (Figure 4(a)), and since the surface is in a constant temperature, the heat transfer rate would be decreased in it. Also, the dissipations cause the fluid to accelerate, and the fluid maximum velocity is increased (Figure 4(b)). The value of the skin friction coefficient is increased by the increase in fluid velocity, which is shown in Figure 5 for pseudoplastic fluids. In Figures 6 and 7, the influence of the generalized Prandtl number is shown in the form of the local Nusselt number and the skin friction coefficient for $\alpha = 0.1$ and Br = 0.5 in the power law model for non-Newtonian fluid with different power law viscosity indices.

By the increase in the generalized Prandtl number, the value of the skin friction coefficient decreases. The reason is that the smaller fluid density causes more sensitivity for the stream caused by buoyancy force, and it thus causes more changes in the wall velocity gradient (Figure 8), and the value of friction factor increases. In other words, with the increase in the Prandtl number, the thickness of the temperature boundary layer decreases, and considering the surface temperature to be constant, the temperature gradient increases (Figure 9), and so does the local Nusselt number.

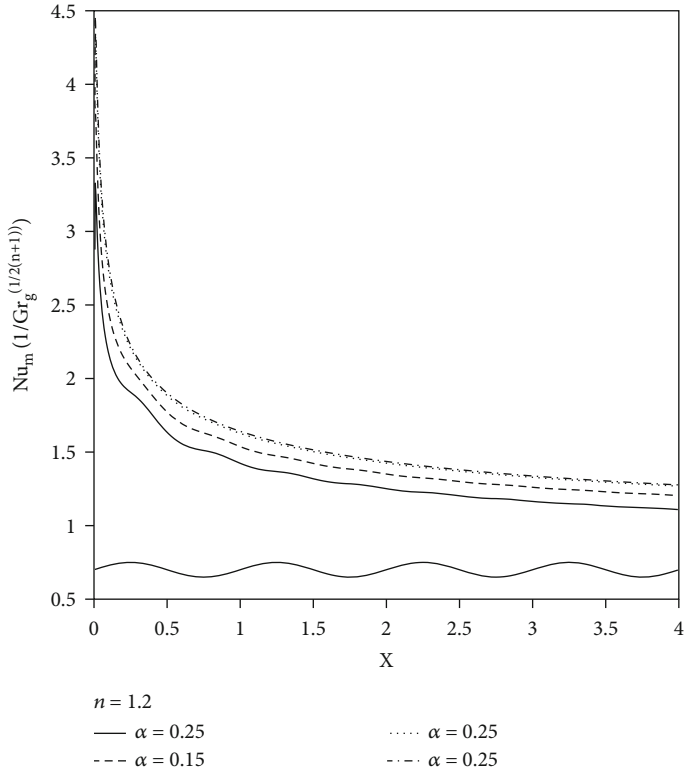

Figure 11: The axial distribution of the mean Nusselt number for $Pr_g = 20$, $Br = 0.7$, $n = 1.2$, and $Q = -0.05$.

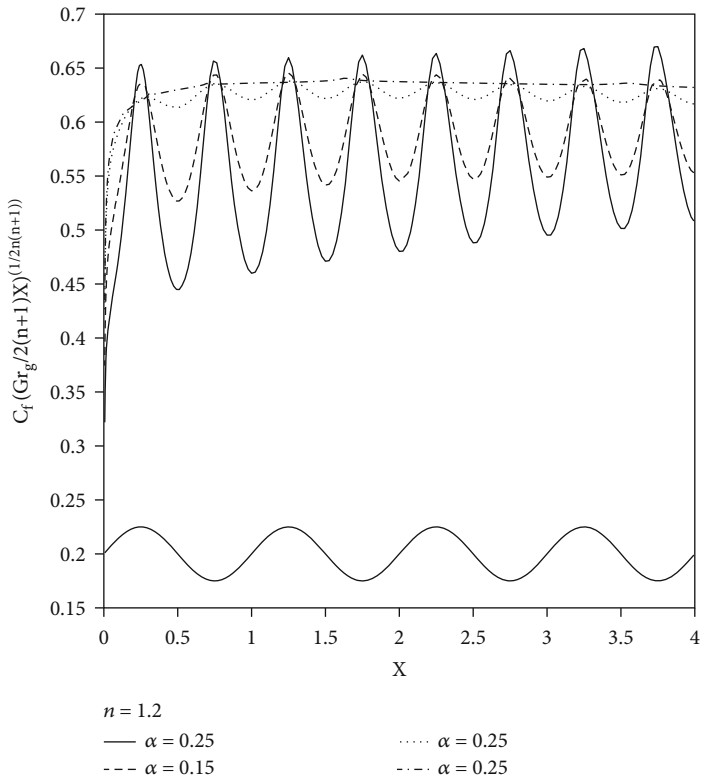

Figure 12: The axial distribution of the skin friction coefficient for $Pr_g = 20$, $Br = 0.7$, $n = 1.2$, and $Q = -0.05$.

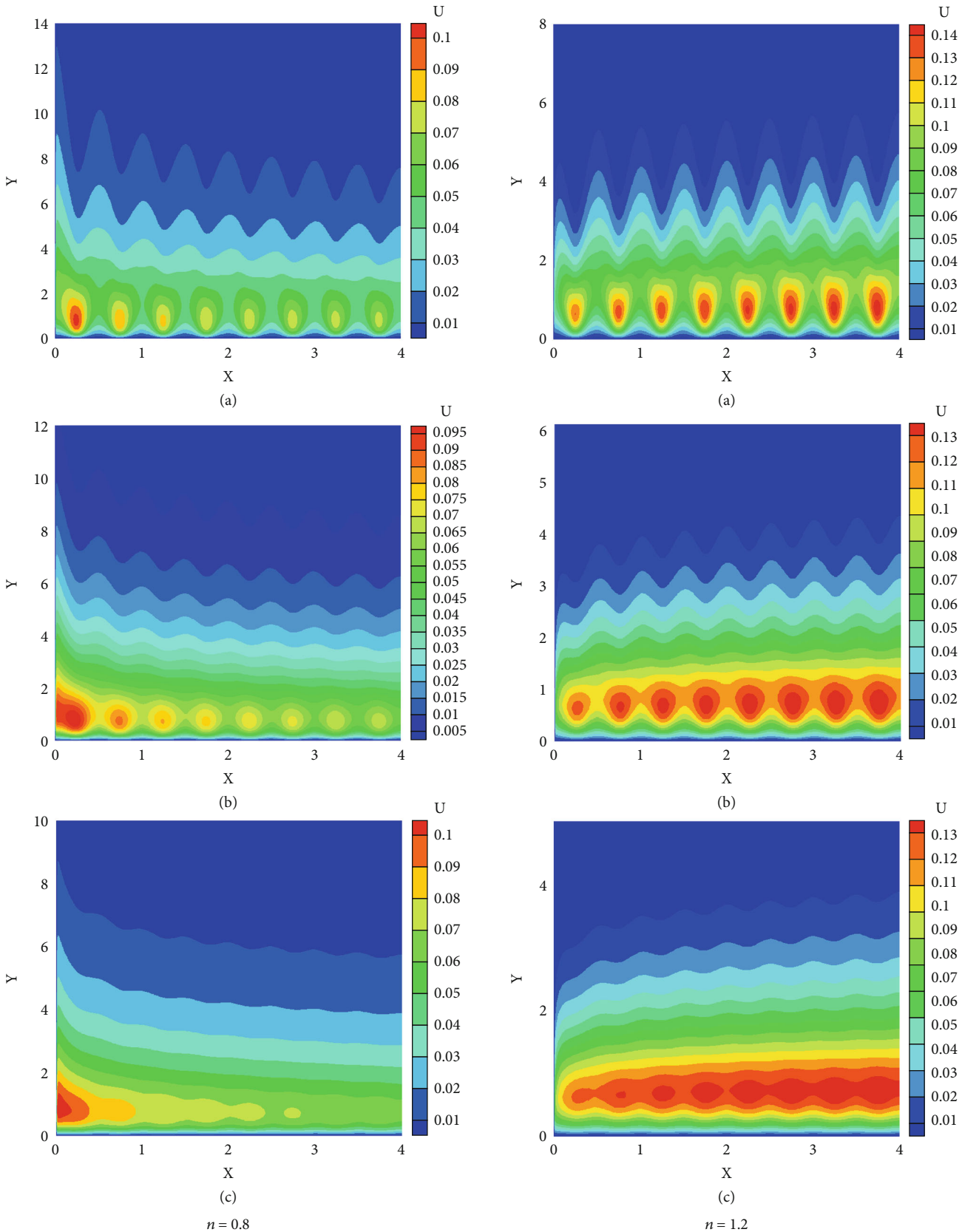

Figure 13: Velocity contour for $Pr_g = 10$, $Br = 0.5$, $n = 0.8$, $Q = -0.05$, $\alpha = 0.2$ (a), $\alpha = 0.1$ (b), and $\alpha = 0.05$ (c).

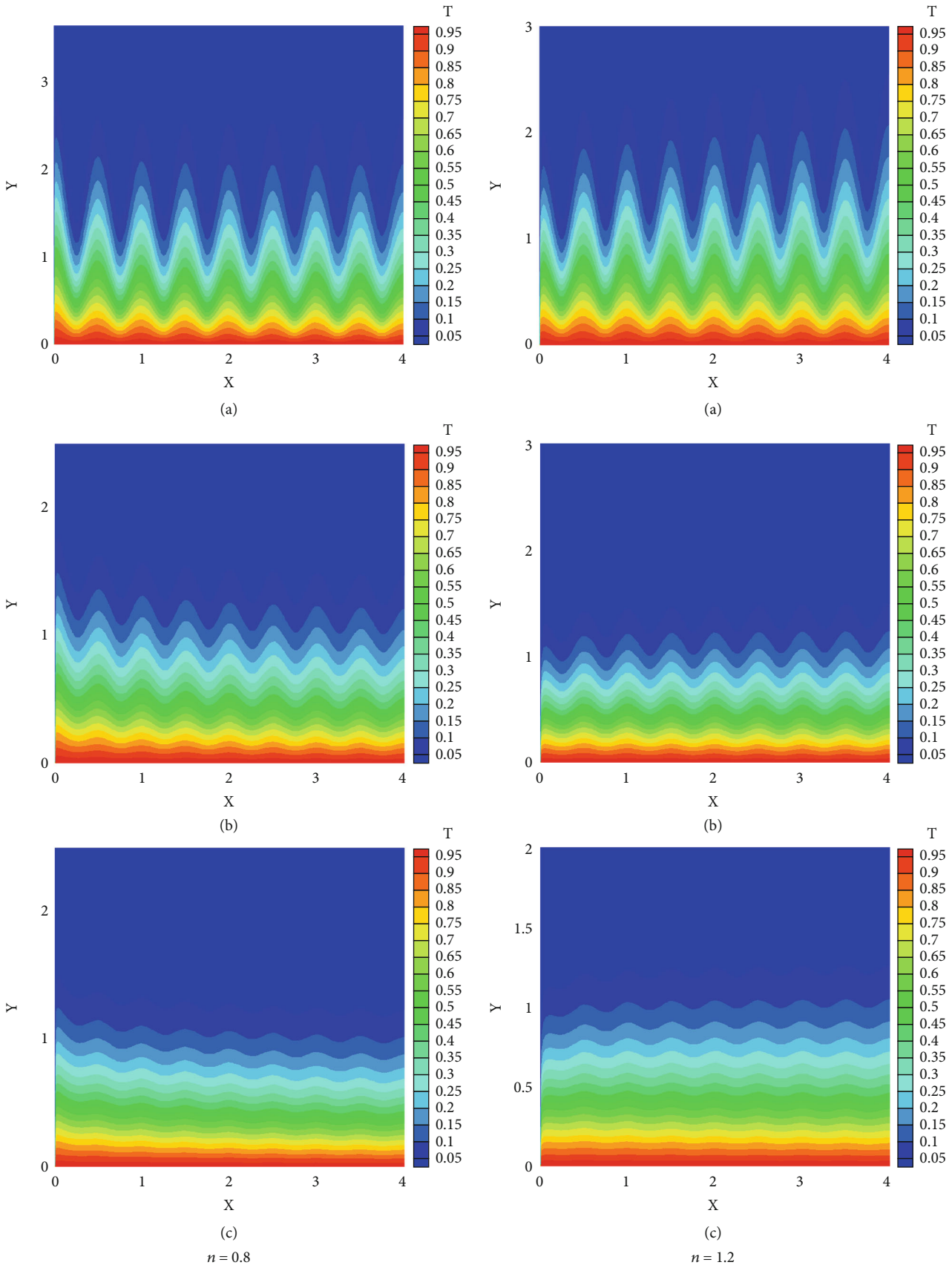

Figure 14: Temperature contour for $Pr_g = 10$, $Br = 0.5$, $n = 0.8$, $Q = -0.05$, $\alpha = 0.2$ (a), $\alpha = 0.1$ (b), and $\alpha = 0.05$ (c).

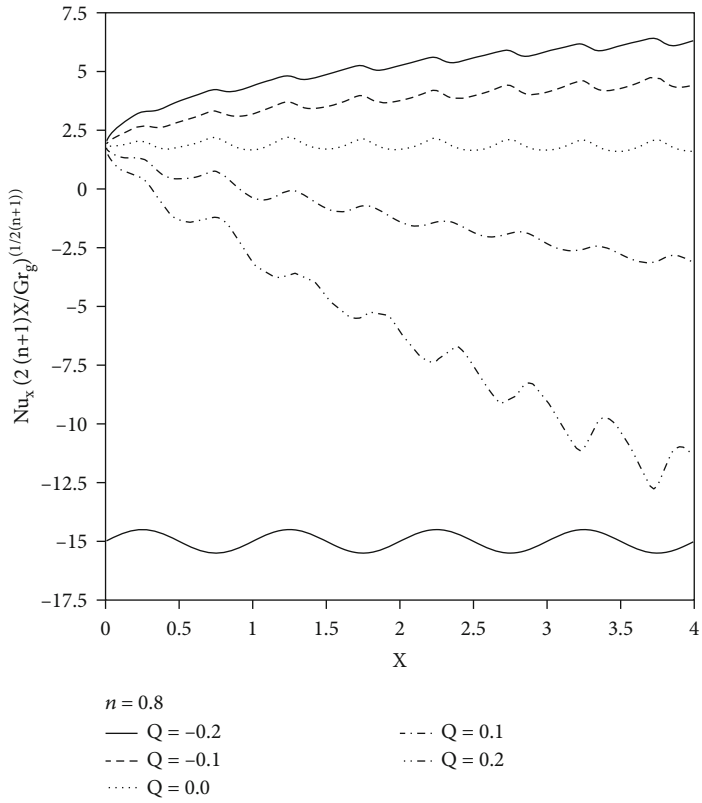

Figure 15: The axial distribution of the local Nusselt number for $Pr_g = 50$, $\alpha = 0.25$, $Br = 0.5$, and $n = 0.8$.

Reviewing the power law viscosity index in Figures 6 and 7, we observe that for dilatant fluid ($n = 1.2$), the local Nusselt number in the vicinity of the plane leading edge has a more value as compared to Newtonian fluid ($n = 1.0$) and to pseudoplastic fluid ($n = 0.8$), whereas its value gradually decreases downstream. Also, in the skin friction coefficient diagram, we observe the contrary of this behavior for a non-Newtonian fluid, and we see that the friction factor for dilatant fluid is less in value than that of Newtonian and pseudoplastic fluids in the plane leading edge, but its value gradually increases downstream.

In Figures 10–12, the influence of the α wavy amplitude wavelength ratio on the diagrams of the local Nusselt number, mean Nusselt number, and skin friction coefficient is shown. The ratio of the local Nusselt number and skin friction coefficient wave amplitude is equal to half of the wavy plane wave amplitude. Furthermore, the oscillation amplitude is increased by the increase in wave amplitude. Also, wave amplitude increases cause decrease in the local Nusselt number and the mean Nusselt number.

Two-dimensional contour of temperature and velocity for non-Newtonian fluid ($n = 0.8$) and dilatant fluid ($n = 1.2$) is depicted in Figures 13 and 14. Grid points at $X = 0.5$, 1, 1.5, and 2 are similar while those at $X = 0.75$, 1.75, and 2.75 correspond to the grid trough and those at $X = 0.25$, 1.25, and 2.25 correspond to the grid crests.

Obviously, the velocity and temperature profile develop periodically along the X direction. It is also seen that the wavelength of the velocity and temperature profile is exactly half of that of the corresponding wavy surface. Considering the dominant term in momentum and energy equations that is multiplied by factor σ'^2 and that σ is a wavy function with waveenght L, as well as σ'^2 having a wavelength of $L/2$, therefore the solution of the equations will be a periodic function with the wavelength $L/2$.

Figures 12 and 13 depict that the hydrodynamic boundary layer and maximum velocity have periodic behaviour in all of the cases. The boundary layer thickness is smaller on troughs and crests compared with around the grid points while the maximum velocity on troughs and crests is higher as compared to the grid points. Moreover, comparing the Figures 13(a)–13(c), one can deduce that increased wave amplitude leads to greater oscillations in the velocity.

4.1. Reviewing the Influence of Heat Generation or Absorption Parameter. In Figures 15 and 16, the effect of heat generation or absorption on the amount of heat transfer is shown as diagrams of local and mean Nusselt numbers. It is observed that the velocity of heat transfer decreases with the increase in heat parameter from the hot surface. Since the heat generation mechanism ($Q > 0.0$) increases the temperature of fluid in the vicinity of the surface and, on the other hand, the temperature of the wall is constant, this decrease is predictable. In other words, when there is heat absorption ($Q < 0.0$), a layer of the cold fluid develops near the hot surface, and therefore, the velocity of heat transfer is increased.

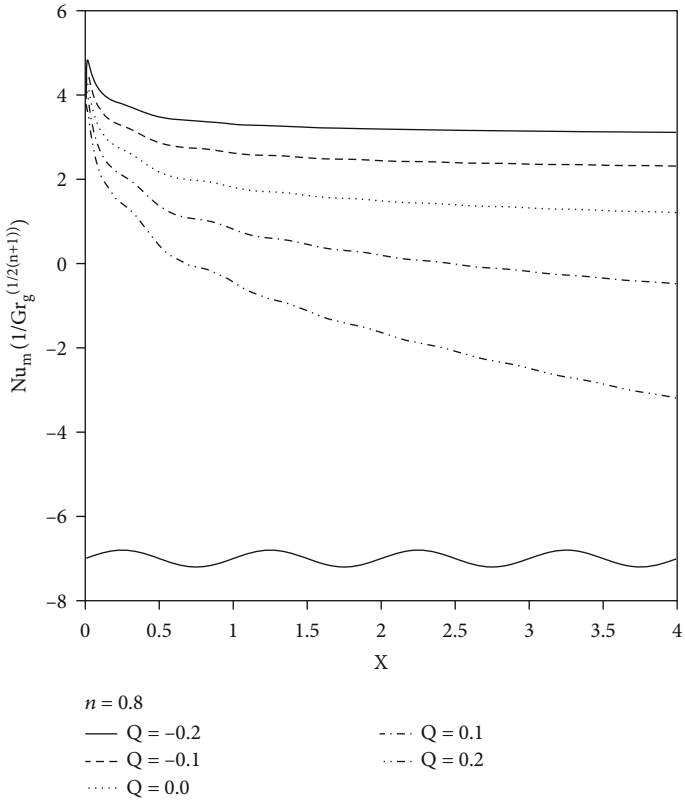

Figure 16: The axial distribution of the mean Nusselt number for $P = 50$, $\alpha = 0.25$, Br = 0.5, and $n = 0.8$.

5. Summary and Conclusions

The effect of viscous dissipation in free convection heat transfer of a non-Newtonian fluid on a vertical wavy surface has been investigated. A simple transform has been used for converting a wavy surface to a smooth one; also, an implicit finite difference numerical solution method has been used for the analysis. The influence of parameters such as the Brinkman no., generalized Prandtl no., wave amplitude magnitude, and power law viscosity index for non-Newtonian fluids has been reviewed as diagrams of the local Nusselt no., mean Nusselt, and friction factor. Summary of the results are represented below:

(1) With the influence of the Brinkman number and the increase in the viscous dissipation amount, the fluid temperature is increased and the amount of heat transfer increased. Also, the fluid velocity is increased

(2) With the increase in the generalized Prandtl number, the local and mean Nusselt numbers increase, but the friction factor decreases. Also, the thickness of the temperature boundary layer decreases

(3) For dilatant fluid, the value of the local Nusselt number is greater as compared to that for Newtonian and pseudoplastic fluids in the vicinity of the plane leading edge, whereas its value gradually decreases downstream

(4) The value of the heat transfer rate decreases with the increase in heat generation parameter from the hot surface, which causes the fluid velocity to increase

Nomenclature

a: Amplitude of wavy surface (m)
Br: Brinkman number
C_f: Skin friction coefficient
C_p: Specific heat of the fluid at constant pressure ($KjKg^{-1}K^{-1}$)
g: Gravitational acceleration (ms^{-2})
Gr_g: Generalized Grashof number ($Wm^{-1}K^{-1}$)
L: Characteristic length (m)
K_P: Nondimensional porous medium parameter, defined by equation
L: Characteristic length (m)
m: Fluid consistency index for power law fluid
n: Power low viscosity index
Nu_x: Local Nusselt number
P: Pressure (Nm^{-2})
Pr_g: Generalized Prandtl number
Q_0: Heat generation or absorption constant ($Wm^{-3}K^{-1}$)
Q: Heat generation or absorption parameter
T: Temperature (K)
V, U: Dimensionless velocity
v, u: Velocity components in the x and y directions, respectively (ms^{-1})

$\tilde{U}$: Characteristic of velocity (ms^{-1})
Y, X: Dimensionless coordinate system
y, x: Coordinate system.

Greeks

β: Thermal expansion coefficient
ρ: Density of fluid ($kg\,m^{-3}$)
σ: Surface geometry function
θ: Dimensionless temperature.

Subscripts

W: Wall surface
∞: Free stream condition.

Data Availability

All the data underlying the findings of the manuscript are available from the corresponding author upon reasonable request.

Conflicts of Interest

The authors declare that they have no conflicts of interest.

References

[1] T.-Y. Wang, "Mixed convection heat transfer from a vertical plate to non-Newtonian fluids," *International Journal of Heat and Fluid Flow*, vol. 16, no. 1, pp. 56–61, 1995.

[2] F. Hady, "Mixed convection boundary-layer flow of non-Newtonian fluids on a horizontal plate," *Applied Mathematics and Computation*, vol. 68, no. 2-3, pp. 105–112, 1995.

[3] Y.-T. Yang, C.'. O. K. Chen, M. T. Lin, and M.-T. Lin, "Natural convection of non-Newtonian fluids along a wavy vertical plate including the magnetic field effect," *International Journal of Heat and Mass Transfer*, vol. 39, no. 13, pp. 2831–2842, 1996.

[4] E. Kim, "Natural convection along a wavy vertical plate to non-Newtonian fluids," *International Journal of Heat and Mass Transfer*, vol. 40, no. 13, pp. 3069–3078, 1997.

[5] C. K. Chen and C. C. Wang, "Transient analysis of forced convection along a wavy surface in micropolar fluids," *Journal of Thermophysics and Heat Transfer*, vol. 14, no. 3, pp. 340–347, 2000.

[6] C.-C. Wang and C.'. K. Chen, "Mixed convection boundary layer flow of non-Newtonian fluids along vertical wavy plates," *International Journal of Heat and Fluid Flow*, vol. 23, no. 6, pp. 831–839, 2002.

[7] J.-H. Jang and W.-M. Yan, "Mixed convection heat and mass transfer along a vertical wavy surface," *International Journal of Heat and Mass Transfer*, vol. 47, no. 3, pp. 419–428, 2004.

[8] M. M. Molla, M. A. Hossain, and L. Shin Yao, "Natural convection flow along a vertical wavy surface with uniform surface temperature in presence of heat generation/absorption," *International Journal of Thermal Sciences*, vol. 43, no. 2, pp. 157–163, 2004.

[9] C.-C. Wang and C.'. K. Chen, "Mixed convection boundary layer flow on inclined wavy plates including the magnetic field effect," *International Journal of Thermal Sciences*, vol. 44, no. 6, pp. 577–586, 2005.

[10] F. Hady, R. Mohamed, and A. Mahdy, "MHD free convection flow along a vertical wavy surface with heat generation or absorption effect," *International Communications in Heat and Mass Transfer*, vol. 33, no. 10, pp. 1253–1263, 2006.

[11] K. Vajravelu and A. Hadjinicolaou, "Heat transfer in a viscous fluid over a stretching sheet with viscous dissipation and internal heat generation," *International Communications in Heat and Mass Transfer*, vol. 20, no. 3, pp. 417–430, 1993.

[12] M. Molla and L. Yao, "Non-Newtonian natural convection along a vertical heated wavy surface using a modified power-law viscosity model," *Journal of Heat Transfer*, vol. 131, no. 1, 2009.

[13] M. Mirzaei Nejad, K. Javaherdeh, and M. Moslemi, "MHD mixed convection flow of power law non-Newtonian fluids over an isothermal vertical wavy plate," *Journal of Magnetism and Magnetic Materials*, vol. 389, pp. 66–72, 2015.

[14] A. Mahdy and S. E. Ahmed, "Unsteady natural convection heat and mass transfer of non-Newtonian Casson fluid along a vertical wavy surface," *International Journal of Mechanical and Mechatronics Engineering*, vol. 11, no. 6, pp. 1284–1291, 2017.

[15] S. Rath and S. K. Dash, "Effect of Prandtl number on natural convection from an isothermal wavy vertical plate in non-Newtonian power-law fluids," in *Twelve International Conference on Thermal Engineering: Theory and Applications*, Gandhinagar, India, 2019.

[16] F. Hady, A. Mahdy, R. Mohamed, S. Ahmed, and O. A. Abozaid, "Unsteady natural convection flow of a dusty non-Newtonian Casson fluid along a vertical wavy plate: numerical approach," *Journal of the Brazilian Society of Mechanical Sciences and Engineering*, vol. 41, no. 11, pp. 1–20, 2019.

[17] M. Kumari, I. Pop, and H. Takhar, "Free-convection boundary-layer flow of a non-Newtonian fluid along a vertical wavy surface," *International Journal of Heat and Fluid Flow*, vol. 18, no. 6, pp. 625–631, 1997.

[18] C.-P. Chiu and H.-M. Chou, "Free convection in the boundary layer flow of a micropolar fluid along a vertical wavy surface," *Acta Mechanica*, vol. 101, no. 1-4, pp. 161–174, 1993.